An Acad Bras Cienc (2024) 96(Suppl. 3): e20230677 DOI 10.1590/0001-3765202420230677
Anais da Academia Brasileira de Ciências | *Annals of the Brazilian Academy of Sciences*
Printed ISSN 0001-3765 I Online ISSN 1678-2690
www.scielo.br/aabc | www.fb.com/aabcjournal

BIOMEDICAL SCIENCES

Lectin-carbohydrate analysis by molecular dynamics: *Parkia* lectins case study

KYRIA S. NASCIMENTO, VINICIUS J.S. OSTERNE, MESSIAS V. OLIVEIRA, JORGE L.C. DOMINGOS, WANDEMBERG P. FERREIRA, ELS J.M. VAN DAMME, BENILDO S. CAVADA & VANIR R. PINTO-JUNIOR

Abstract: Understanding lectin-carbohydrate interactions at the structural and molecular levels is crucial to the field of lectins, as the diverse roles and biological activities exhibited by these proteins are fundamentally linked to their specific binding to target glycoconjugates. This study aimed to apply molecular dynamics to analyze the structure and binding properties of *Parkia* lectins. 3D structures of *Parkia platycephala* and *P. biglobosa* lectins, both unliganded and in complex with D-mannose, were used as inputs for simulations. The trajectories data enabled the study of stability, carbohydrate-binding interactions, and intermonomeric contacts for both proteins. The results revealed stable binding of D-mannose within the lectin domains and their binding mode at each of the three domains, displaying consistent binding motifs across the sites, with slight variations between the lectins and other Jacalin-related lectins. Despite these variations, the binding energies of the lectins with the ligand, as estimated using MM/GBSA, demonstrated favorable interactions in all cases. The dimeric interfaces of both lectins could be identified, and the main contacts have been mapped. These findings enhance our understanding of lectin-carbohydrate interactions and provide insights into the structural properties of *Parkia* lectins for potential biological and therapeutic applications.

Key words: Bioinformatics, lectins, molecular dynamics, *Parkia*.

INTRODUCTION

The study of the structural properties of lectins and their interaction with carbohydrates is at the forefront of the field. Lectins are known to interact with carbohydrates in a specific and reversible way through a shallow cavity in their structures, designated as the carbohydrate-recognition domain (CRD) (Peumans & Van Damme 1995, Weis & Drickamer 1996). Plant lectins are a broad group of well-researched proteins with diverse carbohydrate-binding specificities, biological activities and functional roles (De Coninck & Van Damme 2021). The wide variability of plant lectins allowed their division in 12 families depending on structural features (Van Damme et al. 2008). *Parkia* lectins, the object of the current study, are a member of the mannose-specific subgroup of the jacalin-related lectins. Jacalin-related lectins (JRLs) constitute a diverse family of proteins found in a wide range of organisms. These proteins share a common structural feature, the jacalin domain, named after the lectin that was first identified from Jackfruit (*Artocarpus integrifolia*) (Esch & Schaffrath 2017). JRLs are abundant in plants, particularly those belonging to the Moraceae family. Structurally, the monomers of JRLs typically consist of around 150 residues, folding into a β-prism tertiary structure, containing

three antiparallel β-sheets, each with four strands. These lectins are categorized into two subgroups based on their specificity: galactose-binding and mannose-binding. Unlike the two-chained galactose-binding lectins, mannose-binding jacalin-related lectins typically remain as a single chain but their structure and carbohydrate-binding site composition remain largely similar (Peumans et al. 2000, Bourne et al. 2002). Lectins such as Artocarpin (*Artocarpus heterophyllus*), a lectin specific for D-mannose, and BanLec (*Musa acuminata*), a lectin specific for D-mannose and oligosaccharides containing mannose, are examples of JRLs (Tsaneva & Van Damme 2020).

The *Parkia* genus is part of the Mimosoideae subfamily (Fabaceae family) and, so far, we can find studies about several *Parkia* lectins in the literature, namely: Parkia nitida (Cavada et al. 2023). *Parkia javanica* (PJL) (Utarabhand & Akkayanont 1995), *P. speciosa* (PSL) (Suvachittanont & Peutpaiboon 1992), *P. discolor* (PDL) (Cavada et al. 2000), *P. biglandulosa* (PbiL) (Kaur et al. 2005), *P. pendula* (PpeL) (Coriolano et al. 2014), *P. roxburghii* (PRL) (Kaur et al. 2005), *P. panurensis* (PpaL) (Cavada et al. 2019), *P. biglobosa* (PBL) (Silva et al. 2013, Bari et al. 2016) and *P. platycephala* (PPL) (Mann et al. 2001). These proteins share a high degree of similarity at primary structure level. *Parkia* lectins present a molecular mass ranging between 45-49 kDa containing around ~447 amino acids (Cavada et al. 2020). Only three lectins had their three-dimensional structure experimentally determined by X-ray crystallography. The PPL structure complexed with Xman (5-bromo-4-chloro-3-indolyl-α-D-mannose) was elucidated to a resolution of 2.5 Å and PBL complexed with α-methyl-mannoside was resolved at a resolution of 2.12 Å (Bari et al. 2016). PBL and PPL monomers consist of three β-prism domains tandemly arranged with each one presenting a different CRD. Furthermore, two monomers can associate forming a dimer, resulting in six CRDs for their native structure (Bari et al. 2016, Gallego del Sol et al. 2005). *Parkia* lectins present interesting biological effects such as antinociceptive and anti-inflammatory activity in mice, as well as an antiproliferative effect on lymphoma and hybridoma murine cell lines (Kaur et al. 2005, Silva et al. 2013, Bari et al. 2016). Therefore, understanding the molecular behavior of these proteins when interacting with carbohydrates is important to elucidate the biological mechanism behind these biological activities.

Considering the advancing possibilities with in the application of MD simulations in lectinology, the current work has the goal to provide a case study for molecular dynamics applications to investigate lectin-carbohydrate interactions while contributing to the understanding of *Parkia* lectins. By analyzing the behavior of the lectins, it was possible to observe the dynamics of the interactions between the three different carbohydrate recognition domains of PPL and PBL with D-mannose. Main interactions between the lectins and carbohydrates with particular residues such as an Asp residue occupying the base of the binding site and Tyr residues in the vicinity assisting with stacking interactions are conserved for both lectins. Furthermore, it was possible to observe small structural differences between the binding of the two lectins with unique water bridges allowing the interaction with more distant residues. The trajectory data also allowed the calculation of the theoretical binding energy by MM/GBSA and interaction entropy. The dimeric contacts of both lectins were also analyzed and revealed a remarkable dimeric interface mimicking other JRLs.

The current work provides new insights into the stability and intricate binding details

of two *Parkia* lectins that can provide a more comprehensive understanding of Jacalin-related lectins and their unique properties.

MATERIALS AND METHODS

Hardware

Processor: Intel(R) Core(TM) i9-10850K CPU @ 3.60GHz
GPU: Nvidia 24 Gb RTX 3090 (CUDA-enabled)
RAM: 32 GB DDR4 memory
SSD: 1 TB SSD storage
Operating system: Ubuntu Linux version 20.04

Complex building

In the current case work, molecular docking was applied to obtain the initial coordinates of PBL and PPL complexed with D-mannose (MAN). The coordinates for MAN were retrieved from PubChem, while PBL and PPL coordinates were downloaded from the Protein Data Bank (PDB) using access codes 4mq0 and 1zgs, respectively. Semi-flexible simulations have been set up in GOLD v. 2022.3 with standard settings and ChemPLP as scoring function (Jones et al. 1997, Eldridge et al. 1997). Throughout the simulations, the receptor has remained rigid while the ligand has been allowed flexibility.

The docking algorithm was applied to the center of each carbohydrate-recognition domain and to all residues within a 6 Å radius. Each CRD was evaluated separately, and the best configurations were chosen based on factors such as docking score, hydrogen bonds, nonpolar interactions, and penalty terms for ligand geometry.

Molecular dynamics (MD) simulations

Molecular dynamics simulations were performed for PPL and PBL dimers, both unliganded and bound to MAN. Four different systems were used as inputs for the simulations: unliganded PBL, unliganded PPL, PBL-MAN and PPL-MAN. The files were prepared using the CHARMM-GUI web server (Jo et al. 2008, Lee et al. 2020) and ran under the pmemd.cuda module of the AMBER21 suite (Case et al. 2021) with the parameters of the CHARMM36m force field (Huang et al. 2017). All systems were solvated with the TIP3P water model and neutralized with Na+ counter ions. All systems were subjected to energy minimization steps using a combination of steepest descent and conjugate gradient algorithms with 10 kJ/mol as the convergence criteria. The minimized systems were equilibrated with 500,000 steps (500 ps) of the NVT ensemble followed by the same number of steps under the NPT ensemble. The temperature and pressure of systems were set to 300 K and 1 bar, respectively, and were maintained by a Langevin thermostat and an isotropic Monte-Carlo barostat (Berendsen et al. 1984). MD trajectories totalizing 100 ns (50,000,000 steps) have been produced. The time step for the simulations was set to 2 fs, and the SHAKE algorithm (Ryckaert et al. 1977) was applied to constrain covalent bonds involving hydrogen atoms. The Particle Mesh Ewald (PME) (Essmann et al. 1995) method was used to calculate long-distance electrostatic interactions with a threshold of 10 Å.

Trajectory analysis

The trajectory data were analyzed using Cpptraj (Roe & Cheatham 2013), Xmgrace, and VMD (Humphrey et al. 1996) to extract information for various analyses such as root mean square deviation (RMSD), radius of gyration (RoG), intermolecular hydrogen bonds (H-bonds) and contact frequency. PyMol (Schrödinger, Inc.) was used to generate structure figures. Dimeric contacts using the minimal structure over the course of the simulation have been analyzed through the Protein Interaction Z Score Assessment (PIZSA) server (Roy et al. 2019).

Binding free-energy estimation

One of the main pipelines to estimate binding free energy includes molecular mechanics/ Generalized Born (GB) solvent accessible surface area (MM/GBSA) (Genheden & Ryde 2015, Miller et al. 2012). The binding free energies of the interaction between PPL and PBL with D-mannose has been estimated by this pipeline. The entire trajectory has been used for the calculation according to Equations 1 and 2, as follows:

$$\Delta G_{binding} = G_{complex} - (G_{protein} + G_{ligand}) \quad (1)$$

where $G_{complex}$ is the free energy of the complex, $G_{protein}$ is the free energy of protein, and G_{ligand} is the free energy of ligand, and

$$G = E_{gas} + G_{solvation} - TS \quad (2)$$

where E*gas* refers to molecular mechanics free energy in the gas phase, including the contributions of electrostatic, van der Waals, and internal strain energy. Solvation free energy ΔG_{solv} includes polar (ΔG_{PB}) and nonpolar (ΔG_{SA}) contributions (Eq. 3), as

$$\Delta G_{solv} = \Delta G_{PB} + \Delta G_{SA} \quad (3)$$

GB models were used to estimate the polar contribution. The interior and exterior dielectric constants were set to 1 and 80, respectively. Nonpolar solvation energy was estimated by solvent-accessible surface area (SASA); for this, the surface tension proportionality constant γ was set to 0.00542 kcal × mol$Å^2$, and b, the free energy of nonpolar solvation for a point solute, was set to 0.92 kcal x mol. Sphere radius for SASA calculation was 1.4 Å. After simulation, the energy file was used to generate the binding free value of PPL and PPL with mannose.

Interaction Entropy

In this section, we briefly discuss the Interaction Entropy (IE) method used to obtain the entropic term. Protein-ligand binding free energy (ΔG) can be given by:

$$\Delta G = \Delta G_{gas} + \Delta G_{solv}, \quad (1)$$

where ΔG_{gas} stands for gas-phase free energy, and ΔG_{solv} stands for solvation free energy. Rewriting the gas-phase component (Duan et al. 2016, Sun et al. 2017), we have:

$$\Delta G_{gas} = \frac{1}{\beta}\frac{\int dq_w dq_p dq_l e^{-\beta(E_p+E_l+E_{pl}^{int}+E_w+E_{pw}^{int}+E_{lw}^{int})}}{\int dq_w dq_p dq_l e^{-\beta(E_p+E_l+E_w+E_{pw}^{int}+E_{lw}^{int})}}, \quad (2)$$

where $\beta = 1/k_B T$ and k_B is the Boltzmann constant, T is the absolute temperature, E_p, E_l and E_w are internal energies of the protein, ligand and waters, respectively. $\boldsymbol{E_{pl}^{int}}$ and $\boldsymbol{E_{pw}^{int}}$ are interaction energies of protein-ligand, protein-water and ligand-water, respectively. The protein-ligand interaction incorporates electrostatic and van der Waals interactions. After integration and some mathematical manipulations of Eq. (2), we have:

$$G_{gas} = < E_{pl}^{int} > + k_B T \ln(< e^{\beta \Delta E_{pl}^{int}} >), \quad (3)$$

$$G_{gas} = < E_{pl}^{int} > T\Delta S.$$

Therefore, the IE is defined as:

$$-T\Delta S = k_B T \ln(< e^{\beta \Delta E_{pl}^{int}} >), \quad (4)$$

where ΔE_{pl}^{int} is the fluctuation of protein-ligand interaction energy around the ensemble averaged energy, as defined by

$$\Delta E_{pl}^{int} = E_{pl}^{int} - < E_{pl}^{int} >, \quad (5)$$

where $< E_{pl}^{int} >$ represents the ensemble average of protein-ligand interaction energy, which is given by

$$< E_{pl}^{int} > = \frac{1}{t}\int_0^t (t')dt' E = \frac{1}{N}\sum_{j=1}^{N} E_{pl}^{int}(t_j), \quad (6)$$

where

$$< e^{\Delta E_{pl}^{int}} > = \frac{1}{N}\sum_{j=1}^{N} e^{\beta \Delta E_{pl}^{int}}. \quad (7)$$

Therefore, taking G_{solv} from the MM/PBSA method and G_{gas} obtained by the IE method, we obtain ΔG_{final}.

RESULTS

Molecular docking and MD trajectory analysis

Molecular docking has been performed in the current work to generate the inputs for MD simulations. The scores are summarized in Table I.

The GPU-accelerated pmemd.cuda module of AMBER21 has been used to simulate the dynamics of four systems: unliganded PBL, unliganded PPL, PBL-MAN and PPL-MAN. The simulations ran without issues and no ligands left the binding sites during the trajectory, an indication of specificity and correct ligand parameters.

The time required for the transition of the systems from vacuum to a solvated state was analyzed using RMSD plots (Figure 1a). PBL systems equilibrated very early in the trajectory, with both bound and unbound PBL reaching equilibrium around 20 ns in the simulation. In contrast, for PPL, the unbound system equilibrated much later, at around 60 ns. The carbohydrate-binding appears to have a significant stabilizing effect, causing the system to equilibrate around 20 ns with a lower degree of deviation (2 Å instead of 3.5 Å).

RoG plots were generated to evaluate protein compaction over time and assess the stability of the dimeric system in the presence and absence of the ligand. The data revealed no significant changes, with all systems presenting RoGs in the range of 32 to 33 Å. This suggests that the monomers remained together throughout the simulation, and carbohydrate-binding had no discernible effect on the compaction of the tested lectins. (Figure 1b).

Protein-ligand H-bonds and contact analysis

Hydrogen bonds are the main contributing factor for the interaction between lectins and carbohydrates. Differences in the number of H-bonds lead to variability in carbohydrate-specificity and affinity.

The protein-ligand intermolecular H-bonds plot (Figure 1c) reveals intriguing data regarding the interaction of the different carbohydrate-recognition domains of *Parkia* with carbohydrates. Considering the presence of 3 β-prism domains, each containing a different CRD, per lectin monomer, a closer examination was conducted into each domain and the protein-ligand interactions formed.

The average number of interactions appears to vary per domain, with Domain 1 consistently displaying fewer H-bonds over time, averaging 4.5 bonds, while Domain 2 shows the most interactions, averaging 6 bonds. Domain 3 occupies an intermediate position, with an average of 5 H-bonds consistently formed between the lectins and D-mannose. The superposition of snapshots depicting the binding sites over the course of the MD simulation can be observed in Figure 2a-f. All interactions pointed out in the analysis below have a contact frequency larger than 60% and should be considered nonrandom.

For all three binding sites, D-mannose is held by a combination of H-bonds, π-π stacking interactions, and water bridges. An Asp residue at the base of the sites forms interactions with the O4 and O6 of MAN, along with a stacking interaction with an aromatic residue (Tyr or Phe), and a network of H-bonds formed between O5 and O6 with the backbone of residues found within the loop near the main Asp, hereafter referred to as loop A. Additionally, a contact is formed between the O3 of MAN and a Gly residue in the loop parallel to loop A, which will be referred to as loop B. These interactions remain

Table I. Docking results of PPL and PBL domains interacting with D-mannose (in arbitrary units).

PPL	Final score	Hbond score	Nonpolar score	Buried score	Ligand torsion
Domain 1	-22.41	-5.73	-15.28	-1.40	0.00
Domain 2	-24.81	-7.94	-21.17	4.30	0.00
Domain 3	-27.61	-6.43	-16.61	-4.74	0.17
PBL	**Final score**	**Hbond score**	**Nonpolar score**	**Buried score**	**Ligand torsion**
Domain 1	-29.86	-7.30	-18.13	-4.43	0.00
Domain 2	-36,93	-8.55	-25.35	-3.03	0.00
Domain 3	-32,69	-6.97	-19.71	-6.01	0.00

consistent across the three binding sites and lectins, although some differences are observed.

In Domain 1, Asp140 serves as the base of the binding site, with residues Tyr137 and Tyr138 interacting with loop A, providing further stabilization through π-π stacking interactions. Loop B contains Gly16, forming H-bonds with O4, and the CRD1 of PBL features additional water bridges formed between the O4 of the ligand and the backbone of Leu93 and Tyr137 and O1 of MAN. Moreover, water bridges between Asp17, found on loop B, and the O2 and O3 of MAN were identified. Interestingly, this bridge was not found in PPL.

Domain 2 seems to be more compact and more direct H-bonds have been observed for both lectins. Asp285 in PBL and Asp286 in PPL are at the base of the CRD, Tyr282/283 (PBL) and Tyr283/284 (PPL) can be found on loop A and Gly164 on loop B fulfill the same roles as in CRD1. Not seen in CRD1, Asp165, also on loop B, form direct H-bonds with O2 and O3 of MAN in both lectins and Phe238 (PBL)/Phe239 (PPL) form a parallel stacking interaction with the sugar ring in both lectins. Differences arise in water bridges specific to each lectin, with Gln205 interacting with MAN's O3 in PBL and Glu240 interacting with O4 through a water molecule in PPL.

Domain 3 exhibits a wider structure and slight differences compared to the first two domains. In CRD3, Asp434 (PBL) and Asp435 (PPL) are positioned at the base of the site, with Gly310 (PBL) / Gly311 (PPL) and Asp311 (PBL) / Asp312 (PPL) found on loop B. The Asp residues interact with MAN's O3 through a water bridge. Loop A contains Tyr432 (PBL) / Tyr433 (PPL) and Asp431 (PBL) / Asp432 (PPL), with Tyr residues, akin to the other two CRDs, forming stacking interactions. Additionally, the Asp residues, besides the backbone interaction, directly form a hydrogen bond with the ligand O4. In both lectins, a Phe residue engages in a parallel stacking interaction with the sugar ring.

Binding free-energy estimation

Molecular Mechanics/Generalized Born Surface Area (MM/GBSA) has been employed to evaluate the binding affinities of the two lectins in complex with D-mannose. The binding affinities were calculated across the 3 binding sites. The data revealed that both lectins demonstrated strong intrinsic interactions with the ligand in the gas phase with significantly negative values, this indicates the predominance of favorable non-covalent interactions, as pointed out in section 3.2. The positive solvation energies indicate that unfavorable interactions take place upon solvation, due to disruption of H-bonds

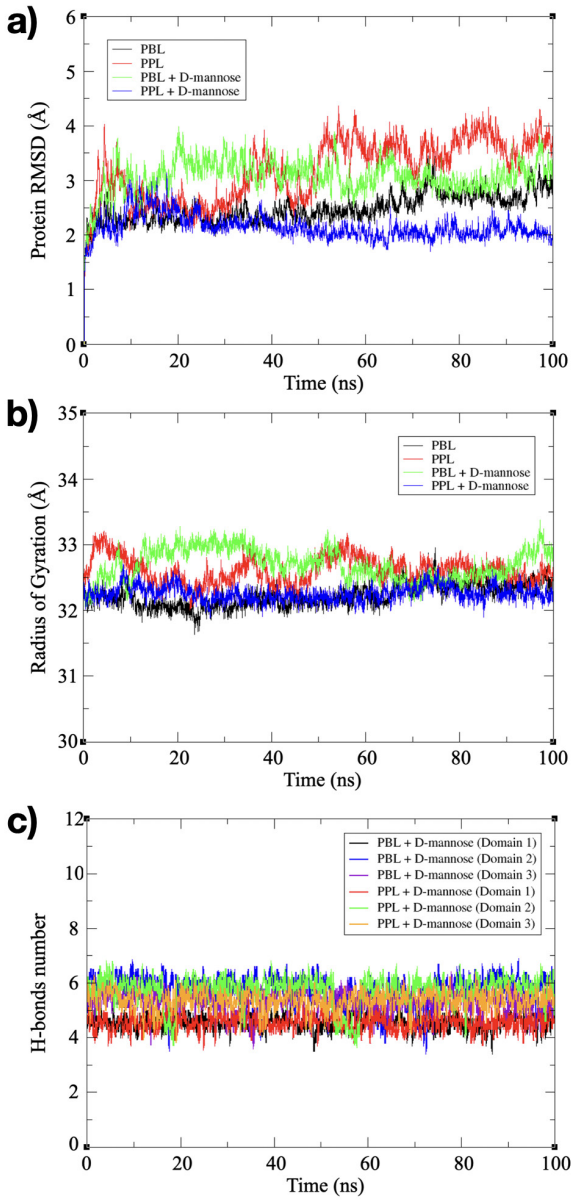

Figure 1. Molecular dynamics trajectory analysis. a) Protein backbone RMSD plots, b) Radius of Gyration plot and c) Plot depicting the hydrogen bonds number between *Parkia* lectin and D-mannose.

and exposure of hydrophobic surfaces caused by the binding. This is in line with what has been shown in the previous section, indicating the presence of hydrophobic residues in the binding site that are exposed within the binding sites.

Positive entropy values at all binding sites suggest that binding is accompanied by a loss of configurational entropy. Notably, the entropy cost was less for PBL at the domain 2, affecting its ΔG_{final} (Table II). For PPL, the total binding energy (ΔG_{total}) showed favorable energetics ranging from -33.54 to -22.25 kcal/mol across the models. After entropy adjustments, the final free energies (ΔG_{final}) were found to be -21.45, -25.09, and -15.82 kcal/mol, respectively. For PBL, similarly, the ΔG_{total} ranged from -31.80 to -26.79 kcal/mol, with ΔG_{final} values of -21.91, -25.76, and -17.32 kcal/mol, respectively.

These findings indicate robust and energetically favorable interactions between both PPL and PBL lectins with D-mannose, with entropic costs being a factor to consider in the overall binding process. The data also suggests slight differences in the efficiency or stability of these interactions, which could be relevant for biological or therapeutic applications involving these lectins.

Dimeric interface analysis

The contacts responsible for the dimer formation in PBL and PPL have been analyzed in detail in the current work. The location of the dimeric interface and the number of bonds formed to stabilize the oligomer are depicted in Figure 3a-c. PIZSA analysis has revealed that the dimeric assembly is stable, and the most important contacts identified are summarized in Table III. The dimers of *Parkia* lectins exhibit two contact points in Domain 1 and Domain 3, interacting with their counterparts in the second monomer. These domains interact in a side-by-side fashion, with the number of contacts varying between the contact points.

DISCUSSION

The goal of the current study was to explore the potential of MD simulations utilizing lectins from *Parkia platycephala* and *P. biglobosa*

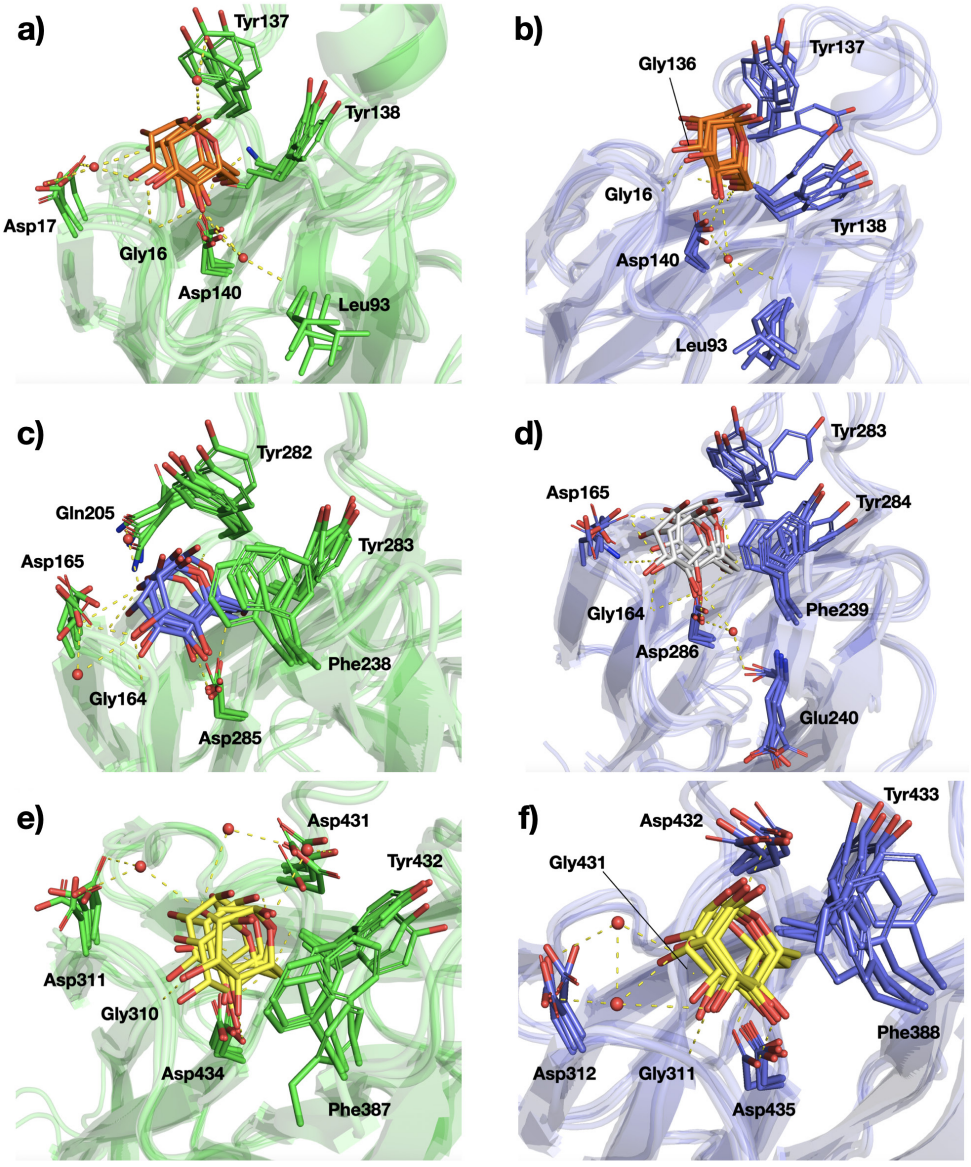

Figure 2. Snapshots of the binding sites of PBL and PPL in complex with D-mannose. a) PBL+D-mannose domain 1, b) PBL+D-mannose domain 2, c) PBL+D-mannose domain 3, d) PPL+D-mannose domain 1, e) PPL+D-mannose domain 2, f) PPL+D-mannose domain 3. The protein is represented as a cartoon in rainbow color, interacting residues and ligands are depicted as sticks. Yellow dashes indicate H-bonds. The superposition contains the snapshots of 0 ns, 25 ns, 50 ns, 75 ns and 100 ns.

as a case study. This research unveils the structural and binding characteristics of *Parkia* lectins, which belong to the underexplored group of *Mimosoideae* lectins. *Parkia* lectins themselves represent an intriguing example of Jacalin-related lectin found in a legume plant. The tertiary structure of JRLs is characterized by a β-prism type I fold consisting of three 4-stranded β-sheets connected by loops and arranged in a triangular structure. Within each β-sheet, a Greek-key motif, composed of four antiparallel β-sheets that loop back on themselves, can be found. This organization allows for the formation of one carbohydrate-recognition domain per β-prism, with the binding site formed between loops at the end of each prism (Tsaneva & Van Damme 2020, Bourne et al. 2002). PPL and PBL contain three β-prisms per monomer, totaling six binding sites within the native protein. Each β-prism aligns with each other with RMSDs varying from 0.8 to 1.2 Å, indicating high structural similarity even with around 50% sequence identity between them (Bari et al. 2016). This structural similarity

Table II. Energy contributions for the interaction of PPL and PBL with D-mannose in kcal/mol.

	MM/GBSA					
	PPL			PBL		
Energy component	**Binding site 1**	**Binding site 2**	**Binding site 3**	**Binding site 1**	**Binding site 2**	**Binding site 3**
ΔG_{gas}	-71.69± 4.75	-77.23 ± 5.11	-64.12 ± 5.35	-87.71 ± 6.32	-73.12 ± 2.65	-70.92 ± 5.02
ΔG_{solv}	40.28 ± 2.78	43.69 ± 3.77	41.87 ± 4.14	55.91 ± 2.89	43.56 ± 2.12	45.38 ± 3.78
ΔG_{total}	-31.41 ± 2.63	-33.54 ± 2.75	-22.25 ± 2.38	-31.80 ± 2.71	-26.79 ± 2.73	-29.52 ± 2.89
Entropy	9.94	8.45	6.43	9.89	3.08	8.22
ΔG_{final}	-21.45 ± 2.63	-25.09 ± 2.75	-15.82 ± 2.38	-21.91 ± 2.71	-25.76 ± 2.73	-17.32 ± 2.89

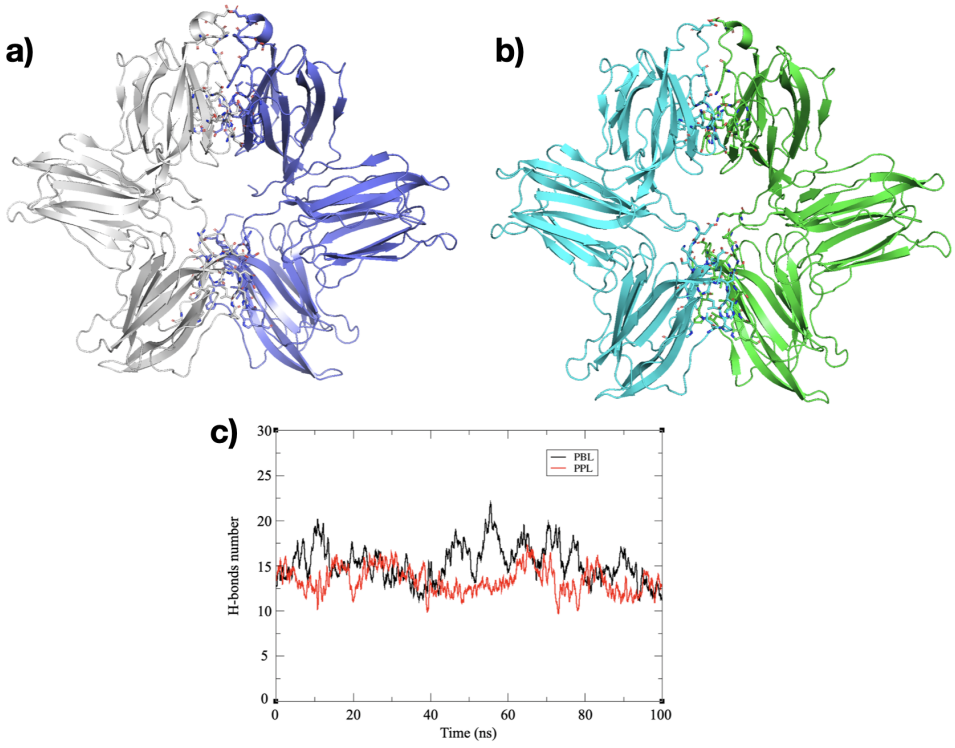

Figure 3. Dimeric interface of the lectins. a) 3D structure of PBL with residues within the dimeric interface represented as sticks. b) 3D structure of PBL with residues within the dimeric interface represented as sticks. c) Number of H-bonds responsible for holding the oligomeric structures over the course of the simulation.

is not surprising, considering that plant JRLs can vary from single domain proteins to multiple domains tandemly arranged (Han et al. 2018, Bourne et al. 1999). Furthermore, these lectins can contain additional domains such as dirigent and Kelch domains, forming chimerolectins (Xiang et al. 2011).

All simulations reached equilibrium at different time-points. The time for a system to shift from an energy-minimized state to a fully solvated condition depends on several factors including the degree of minimization, the solvent used, inherent properties of the protein, presence or absence of ligands, etc. Equilibration

Table III. Non-exhaustive list of interacting interface residues, ranked by interaction favorability.

PBL	PPL
Phe54 A - Gly52 B	Gly304 A - Pro417 B
Gly52 A - Phe54 B	Gly299 - Pro443 B
Asp17 A - Ile 50 B	Tyr18 A - Ile50 B
Ile50 A - Asp 17 B	Phe54 A - Ser51 B
Glu61 A - Glu61 B	Ser51 A - Phe54 B
Ile300 A - Ile300 B	Pro417 A - Gly304 B
Gly303 A - Pro416 B	Ser300 A - Asn420 B
Pro416 A - Gly303 B	Tyr18 A - Asp49 B
Gly303 A - His418 B	Asp49 A - Tyr18 B
His418 A - Gly303 B	Ile303 A - Pro417 B

times vary between proteins and simulations, but it is generally accepted that binding with ligands may help to accelerate the process, a fact that has been observed for PPL, but not for PBL (Figure 1a). The observed differences in equilibration times between PBL and PPL, for both their bound and unbound forms, are likely due to intrinsic properties of the proteins and their interactions with the ligand. The faster equilibration of PBL in both liganded and unliganded forms indicates an inherently more stable structure compared to PPL, which shows significant stabilization upon ligand binding. This implies that PPL's structure is more sensitive to ligand presence, possibly due to higher intrinsic flexibility that is reduced by specific ligand-protein interactions. These interactions involve critical stabilizing forces such as hydrogen bonds or hydrophobic contacts, which reduce conformational entropy and lead to a more rigid structure in the ligand-bound state. Interaction with specific ligands usually has a stabilizing effect on the protein structure and can be a direct indication of a specific ligand (Mazal et al. 2018). The comparison of unliganded lectins with complexes can provide insight into protein stability and the effect of binding on specific regions of the structure. Stabilizing effects in the presence of ligands have been observed for other lectins, such as *Dioclea lasiophylla* lectin during MD simulations (Pinto-Junior et al. 2017).

The analysis of the interactions between *Parkia* lectins and D-mannose revealed an overall conserved binding motif with unique variations within each site demonstrating the uniqueness of lectin-carbohydrate binding. The average number of protein-ligand H-bonds varied slightly per domain which, although interesting, should be analyzed carefully since water bridges have an important participation and appear to be unique between lectins and especially important in wider binding sites, namely CRD 1 and CRD 3, where water molecules allow H-bonds with an extra Asp residue. The intricate binding profile explained in section 3.2 led to significantly negative values in the MM/GBSA analysis, an indication of high affinity. High negative values in the gas phase underscore the importance of non-covalent interactions, the main contributors for lectin-carbohydrate binding (Osterne et al. 2024), solvation and positive entropic negatively affected the binding.

The binding profile of JRLs is known for a long time, the binding of mannose-specific JRLs follow the same overall principles with some properties being shared between virtually all lectins of this group. These include the Asp residue forming interactions with the O4 and

O6 hydroxyl groups of mannosides, a network of H-bonds with the backbone of residues on loop A and the contacts with a conserved Gly on loop B (Azarkan et al. 2018, Bourne et al. 2002). The residues within loop A are not conserved and vary per protein with some forming additional H-bonds with the ligand, normally at the O2 of MAN as seen in the banana lectin (BanLec) (Figure 4). The binding between *Parkia* lectins and D-mannose adds some non-covalent interactions in comparison to other JRLs, these include several π-π stacking interactions not commonly found in representative lectins such as Artocarpin and BanLec (Figure 4). Overall, PBL and PPL introduce several aromatic residues in their binding sites, and this can lead to stronger affinities with the ligand (Zhang et al. 2021, García-Hernández et al. 2000). The overall shallowness of *Parkia* CRDs may indicate a small number of extended binding site residues and a preference for terminal regions considering the steric clashes with several Tyr residues that may take place with larger glycans. This is unlike what is observed with other JRLs including Orysata and Artocarpin, both lectins that have the core Man3GlcNAc2 as one of their main binding epitopes according to glycan array data (Al Atalah et al. 2011, Bojar et al. 2022, Jeyaprakash et al. 2004).

The interactions stabilizing the dimeric structure involve amino acids from domains 1 and 3. The overall interface is quite similar when comparing the two lectins, although small differences have been observed in the contacts, the residues forming the contact pairs are largely similar, with the differences in pairs possibly being observed due to the dynamic nature of the interface and the snapshot corresponding to the average structure. Nonetheless, it can be concluded that both lectins follow the same side-by-side dimer profile, with the Domain 3 - Domain 3 contact point presenting the commonly found 15° tilt of one subunit relative to the other (Sharma & Vijayan 2011) and the Domain 1 - Domain 1 contact point presenting a more angular side-by-side organization slightly

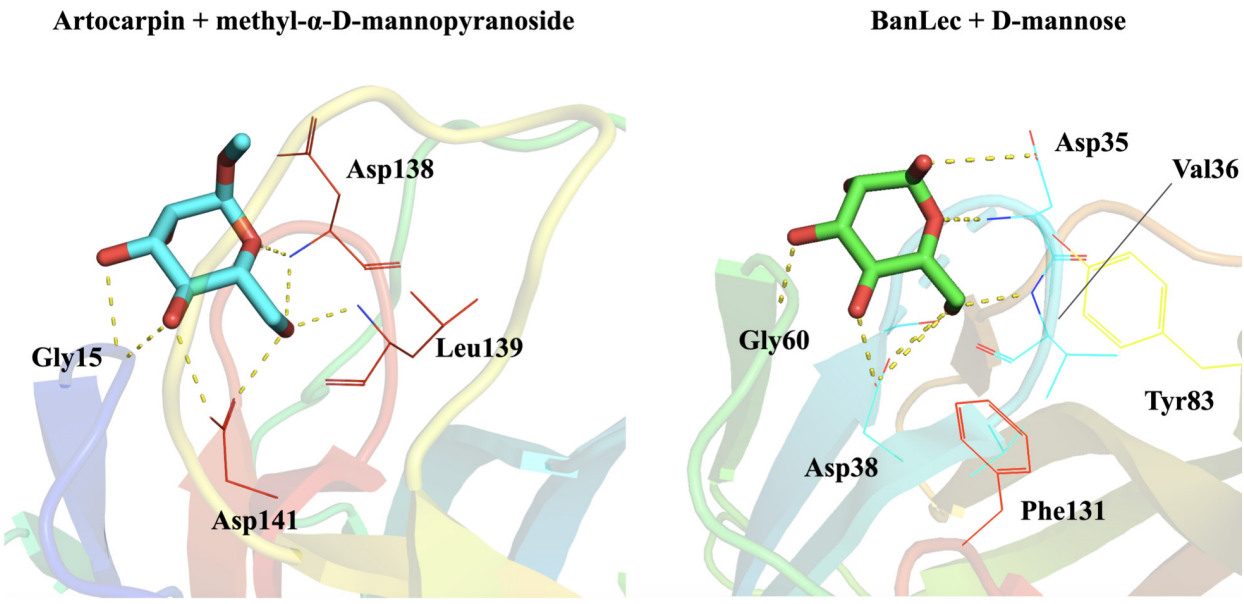

Figure 4. Binding mode of Artocarpin (PDB id: 1j4u) and the Banana lectin (PDB id: 3mit) with ligands. Proteins are depicted as cartoons in rainbow colors, and interacting residues are illustrated as lines. Ligands are represented as sticks, with yellow dashes indicating H-bonds.

different from Jacalin. This side-by-side dimeric profile is observed in several tetrameric JRLs, as well as in the octameric Heltuba (Bourne et al. 1999, Abhinav & Vijayan 2014). Additionally, the *Parkia* dimers demonstrated to be quite stable over the course of the MD trajectory with no signs of collapse.

Thus, we can conclude that *Parkia* lectins are stable proteins whose binding follows the same overall principles as other JRLs, although several important differences could be observed which likely lead to stronger binding due to additional interactions not previously identified in the crystal structure. The MD analysis presented here provides a nice framework for predicting lectin binding, offering important information for lectin-based applications. The identification of binding modes and motifs contributes to the lectinology field and is a crucial aspect for the study of these proteins. This understanding may pave the way for the engineering of binding sites and the construction of chimera lectins using specific domains aimed at exploiting the unique properties of *Parkia* lectins for potential biological and therapeutic applications.

Acknowledgments

This study was supported by grants from the Conselho Nacional de Desenvolvimento Científico e Tecnológico (CNPq), Coordenação de Aperfeiçoamento de Pessoal de Nível Superior (CAPES) and Fundação Cearense de Apoio ao Desenvolvimento Científico e Tecnológico (FUNCAP). B.S.C., K.S.N. and W.P.F are senior investigators of CNPq. VJSO thanks FWO-Vlaanderen for the postdoctoral fellowship (12T4622N). David Martin helped with the English editing of the manuscript.

REFERENCES

ABHINAV KV & VIJAYAN M. 2014. Structural diversity and ligand specificity of lectins. The Bangalore effort. J Macromol Sci Part A Pure Appl Chem 86: 1335-1355.

AL ATALAH B, FOUQUAERT E, VANDERSCHAEGHE D, PROOST P, BALZARINI J, SMITH DF, ROUGÉ P, LASANAJAK Y, CALLEWAERT N & VAN DAMME EJM. 2011. Expression analysis of the nucleocytoplasmic lectin "Orysata" from rice in *Pichia pastoris*. FEBS J 278: 2064-2079.

AZARKAN M, FELLER G, VANDENAMEELE J, HERMAN R, EL MAHYAOUI R, SAUVAGE E, VANDEN BROECK A, MATAGNE A, CHARLIER P & KERFF F. 2018. Biochemical and structural characterization of a mannose binding jacalin-related lectin with two-sugar binding sites from pineapple (Ananas comosus) stem. Sci Rep 8: 11508.

BARI AU ET AL. 2016. Lectins from *Parkia biglobosa* and *Parkia platycephala*: A comparative study of structure and biological effects. Int J Biol Macromol 92: 194-201.

BERENDSEN HJC, POSTMA JPM, VAN GUNSTEREN WF, DINOLA A & HAAK JR. 1984. Molecular dynamics with coupling to an external bath. J Chem Phys 81: 3684-3690.

BOJAR D, MECHE L, MENG G, ENG W, SMITH DF, CUMMINGS RD & MAHAL LK. 2022. A Useful Guide to Lectin Binding: Machine-Learning Directed Annotation of 57 Unique Lectin Specificities. ACS Chem Biol 17: 2993-3012.

BOURNE Y, ASTOUL CH, ZAMBONI V, PEUMANS WJ, MENU-BOUAOUICHE L, VAN DAMME EJM, BARRE A & ROUGÉ P. 2002. Structural basis for the unusual carbohydrate-binding specificity of jacalin towards galactose and mannose. Biochem J 364: 173-180.

BOURNE Y, ZAMBONI V, BARRE A, PEUMANS WJ, VAN DAMME EJ & ROUGÉ P. 1999. *Helianthus tuberosus* lectin reveals a widespread scaffold for mannose-binding lectins. Structure 7: 1473-1482.

CASE ET AL. 2021. Amber 2021, University of California, San Francisco, 957 p.

CAVADA BS ET AL. 2000. Purification, chemical, and immunochemical properties of a new lectin from Mimosoideae (*Parkia discolor*). Prep Biochem Biotechnol 30: 271-280.

CAVADA BS ET AL. 2019. Purification and partial characterization of a new lectin from *Parkia panurensis* Benth. ex H.C. Hopkins seeds (Leguminosae family; Mimosoideae subfamily) and evaluation of its biological effects. Int J Biol Macromol 145: 845-855.

CAVADA BS, BARI AU, PINTO-JUNIOR VR, OLIVEIRA MV, MACHADO PIM, SOUZA LAG, NASCIMENTO KS & OSTERNE VJS. 2023. Biochemical and structural properties of a lectin purified from seeds of the legume *Parkia nitida* Miq. Proc Biohem 132: 337-345.

CAVADA BS, OSTERNE VJS, OLIVEIRA MV, PINTO-JUNIOR VR, SILVA MTL, BARI AU, LIMA LD, LOSSIO CF & NASCIMENTO KS. 2020. Reviewing Mimosoideae lectins: A group of under explored legume lectins. Int J Biol Macromol 154: 159-165.

DE CONINCK T & VAN DAMME EJM. 2021. Review: The multiple roles of plant lectins. Plant Sci 313: 111096.

DUAN L, LIU X & ZHANG JZH. 2016. Interaction Entropy: A New Paradigm for Highly Efficient and Reliable Computation of Protein-Ligand Binding Free Energy. J Am Chem Soc 138: 5722-5728.

ELDRIDGE MD, MURRAY CW, AUTON TR, PAOLINI GV & MEE RP. 1997. Empirical scoring functions: I. The development of a fast empirical scoring function to estimate the binding affinity of ligands in receptor complexes. J Comput Aided Mol Des 11: 425-445.

ESCH L & SCHAFFRATH U. 2017. An Update on Jacalin-Like Lectins and Their Role in Plant Defense. Int J Mol Sci 18: 1592.

ESSMANN U, PERERA L, BERKOWITZ ML, DARDEN T, LEE H & PEDERSEN LG. 1995. A smooth particle mesh Ewald method. J Chem Phys 103: 8577-8593.

GALLEGO DEL SOL F, NAGANO C, CAVADA BS & CALVETE JJ. 2005. The first crystal structure of a Mimosoideae lectin reveals a novel quaternary arrangement of a widespread domain. J Mol Biol 353: 574-583.

GARCÍA-HERNÁNDEZ E, ZUBILLAGA RA, RODRÍGUEZ-ROMERO A & HERNÁNDEZ-ARANA A. 2000. Stereochemical metrics of lectin-carbohydrate interactions: comparison with protein-protein interfaces. Glycobiology 10: 993-1000.

GENHEDEN S & RYDE U. 2015. The MM/PBSA and MM/GBSA methods to estimate ligand-binding affinities. Expert Opin Drug Discov 10: 449-461.

HAN Y-J, ZHONG Z-H, SONG L-L, STEFAN O, WANG Z-H & LU G-D. 2018. Evolutionary analysis of plant jacalin-related lectins (JRLs) family and expression of rice JRLs in response to Magnaporthe oryzae. J Integr Agric 17: 1252-1266.

HUANG J, RAUSCHER S, NAWROCKI G, RAN T, FEIG M, DE GROOT BL, GRUBMÜLLER H & MACKERELL JR AD. 2017. CHARMM36m: an improved force field for folded and intrinsically disordered proteins. Nat Methods 14: 71-73.

HUMPHREY W, DALKE A & SCHULTEN K. 1996. VMD: visual molecular dynamics. J Mol Graph 14: 33-38.

JEYAPRAKASH AA, SRIVASTAV A, SUROLIA A & VIJAYAN M. 2004. Structural basis for the carbohydrate specificities of artocarpin: variation in the length of a loop as a strategy for generating ligand specificity. J Mol Biol 338: 757-770.

JO S, KIM T, IYER VG & IM W. 2008. CHARMM-GUI: a web-based graphical user interface for CHARMM. J Comput Chem 29: 1859-1865.

JONES G, WILLETT P, GLEN RC, LEACH AR & TAYLOR R. 1997. Development and validation of a genetic algorithm for flexible docking. J Mol Biol 267: 727-748.

KAUR N, SINGH J, KAMBOJ SS, AGREWALA JN & KAUR M. 2005. Two novel lectins from *Parkia biglandulosa* and *Parkia roxburghii*: isolation, physicochemical characterization, mitogenicity and anti-proliferative activity. Protein Pept Lett 12: 585-595.

LEE J, HITZENBERGER M, RIEGER M, KERN NR, ZACHARIAS M & IM W. 2020. CHARMM-GUI supports the Amber force fields. J Chem Phys 153: 035103.

MANN K, FARIAS CM, DEL SOL FG, SANTOS CF, GRANGEIRO TB, NAGANO CS, CAVADA BS & CALVETE JJ. 2001. The amino-acid sequence of the glucose/mannose-specific lectin isolated from *Parkia platycephala* seeds reveals three tandemly arranged jacalin-related domains. Eur J Biochem 268: 4414-4422.

MAZAL H, AVIRAM H, RIVEN I & HARAN G. 2018. Effect of ligand binding on a protein with a complex folding landscape. Phys Chem Chem Phys 20: 3054-3062.

MILLER BR III, MCGEE JR TD, SWAILS JM, HOMEYER N, GOHLKE H & ROITBERG AE. 2012. MMPBSA.py: An Efficient Program for End-State Free Energy Calculations. J Chem Theory Comput 8: 3314-3321.

OSTERNE VJS, PINTO-JUNIOR VR, OLIVEIRA MV, NASCIMENTO KS, VAN DAMME EJM & CAVADA BS. 2024. Computational insights into the circular permutation roles on ConA binding and structural stability. Curr Res Struct Biol 7: 100140.

PEUMANS WJ, HAUSE B & VAN DAMME EJ. 2000. The galactose-binding and mannose-binding jacalin-related lectins are located in different sub-cellular compartments. FEBS Lett 477: 186-192.

PEUMANS WJ & VAN DAMME EJM. 1995. Lectins as Plant Defense Proteins. Plant Physiol 109: 347-352.

PINTO-JUNIOR VR ET AL. 2017. Molecular modeling, docking and dynamics simulations of the *Dioclea lasiophylla* Mart. Ex Benth seed lectin: An edematogenic and hypernociceptive protein. Biochimie 135: 126-136.

ROE DR & CHEATHAM TE III. 2013. PTRAJ and CPPTRAJ: Software for Processing and Analysis of Molecular Dynamics Trajectory Data. J Chem Theory Comput 9: 3084-3095.

ROY AA, DHAWANJEWAR AS, SHARMA P, SINGH G & MADHUSUDHAN MS. 2019. Protein Interaction Z Score Assessment (PIZSA): an empirical scoring scheme for evaluation of protein-protein interactions. Nucleic Acids Res 47: W331-W337.

RYCKAERT J-P, CICCOTTI G & BERENDSEN HJC. 1977. Numerical integration of the cartesian equations of motion of a system with constraints: molecular dynamics of n-alkanes. J Comput Phys 23: 327-341.

SHARMA A & VIJAYAN M. 2011. Quaternary association in beta-prism I2 fold plant lectins: insights from X-ray crystallography, modelling and molecular dynamics. J Biosci 36: 793-808.

SILVA HC ET AL. 2013. Purification and primary structure of a mannose/glucose-binding lectin from *Parkia biglobosa* Jacq. seeds with antinociceptive and anti-inflammatory properties. J Mol Recognit 26: 470-478.

SUN Z, YAN YN, YANG M & ZHANG JZH. 2017. Interaction entropy for protein-protein binding. J Chem Phys 146: 124124.

SUVACHITTANONT W & PEUTPAIBOON A. 1992. Lectin from *Parkia speciosa* seeds. Phytochemistry 31: 4065-4070.

TSANEVA M & VAN DAMME EJM. 2020. 130 years of Plant Lectin Research. Glycoconj J 37: 533-551.

UTARABHAND P & AKKAYANONT P. 1995. Purification of a lectin from *Parkia javanica* beans. Phytochemistry 38: 281-285.

VAN DAMME EJM, LANNOO N & PEUMANS WJ. 2008. Plant Lectins. In: KADER J-C & DELSENY M (Eds), Advances in Botanical Research, Academic Press, p. 107-209.

WEIS WI & DRICKAMER K. 1996. Structural basis of lectin-carbohydrate recognition. Annu Rev Biochem 65: 441-473.

XIANG Y, SONG M, WEI Z, TONG J, ZHANG L, XIAO L, MA Z & WANG Y. 2011. A jacalin-related lectin-like gene in wheat is a component of the plant defence system. J Exp Bot 62: 5471-5483.

ZHANG S, CHEN KY & ZOU X. 2021. Carbohydrate-Protein Interactions: Advances and Challenges. Commun Inf Syst 21: 147-163.

How to cite

NASCIMENTO KS, OSTERNE VJS, OLIVEIRA MV, DOMINGOS JLC, FERREIRA WP, VAN DAMME EJM, CAVADA BS & PINTO-JUNIOR VR. 2024. Lectin-carbohydrate analysis by molecular dynamics: *Parkia* lectins case study. An Acad Bras Cienc 96: e20230677. DOI 10.1590/0001-3765202420230677.

Manuscript received on June 14, 2023;
accepted for publication on September 16, 2024

KYRIA S. NASCIMENTO[1]
https://orcid.org/0000-0002-2220-4552

VINICIUS J.S. OSTERNE[1,2]
https://orcid.org/0000-0002-5730-8829

MESSIAS V. OLIVEIRA[1]
https://orcid.org/0000-0003-4754-7743

JORGE L.C. DOMINGOS[3]
https://orcid.org/0000-0003-0492-8693

WANDEMBERG P. FERREIRA[3]
https://orcid.org/0000-0001-8262-237X

ELS J.M. VAN DAMME[2]
https://orcid.org/0000-0001-9848-766X

BENILDO S. CAVADA[1]
https://orcid.org/0000-0002-5791-6170

VANIR R. PINTO-JUNIOR[1,3]
https://orcid.org/0000-0002-9279-5298

[1]Universidade Federal do Ceará, Departamento de Bioquímica e Biologia Molecular, Laboratório de Moléculas Biologicamente Ativas, Rua José Aurelio Camara, s/n, 60440-970 Fortaleza, CE, Brazil

[2]Ghent University, Department of Biotechnology, Laboratory of Biochemistry and Glycobiology, Proeftuinstraat 86, 9000 Ghent, Belgium

[3]Universidade Federal do Ceará, Departamento de Física, Rua José Aurelio Camara, s/n, 60440-970 Fortaleza, CE, Brazil

Correspondence to: **Kyria Santiago Nascimento, Vanir Reis Pinto-Junior**
E-mail: kyriasantiago@ufc.br, vanirjr.ufc@gmail.com

Author contributions

Kyria S. Nascimento: Conceptualization, Investigation, Project administration, Validation, Formal analysis, Resources, Supervision, Funding acquisition, Writing—original draft, Writing—review & editing. Vinicius J.S. Osterne: Methodology; Validation; Formal analysis; Funding acquisition; Writing—original draft, Writing—review & editing. Messias V. Oliveira and Jorge L.C. Domingos: Methodology; Validation; Formal analysis; Writing—original draft, Writing—review & editing. Wandemberg P. Ferreira: Methodology; Validation; Formal analysis; Supervision, Writing—review & editing. Els J.M. Van Damme: Validation; Formal analysis; Supervision, Resources, Writing—review & editing. Benildo S. Cavada: Validation; Formal analysis; Supervision, Resources, Funding acquisition, Writing—review & editing. Vanir R. Pinto-Junior: Conceptualization, Investigation, Methodology, Validation, Formal analysis, Supervision, Writing—original draft, Writing—review & editing.